PASSIVE UHF RFID-ENABLED SENSOR SYSTEM FOR DETECTION OF PRODUCT'S EXPOSURE TO ELEVATED TEMPERATURE

Kamil Janeczek[1], Małgorzata Jakubowska[2,3], Grażyna Kozioł[1], Piotr Jankowski-Mihułowicz[4]

1) *Tele and Radio Research Institute, 11 Ratuszowa Street, 03-450 Warsaw, Poland (✉ kamil.janeczek@itr.org.pl, +48 226192241)*
2) *Institute of Electronic Materials Technology, 133 Wolczynska Street, 01-919 Warsaw, Poland*
3) *Warsaw University of Technology, Institute of Metrology and Biomedical Engineering, 8 Sankt Andrzej Bobola Street, 02-525 Warsaw, Poland*
4) *Rzeszów University of Technology, Department of Electronic and Communications Systems, 2 Wincenty Pol Street, 35-959 Rzeszów, Poland*

Abstract

Temperature change is one of key factors which should be taken into account in logistics during transportation or storage of many types of goods. In this study, a passive UHF RFID-enabled sensor system for elevated temperature (above 58°C) detection has been demonstrated. This system consists of an RFID reader and disposable temperature sensor comprising an UHF antenna, chip and temperature sensitive unit. The UHF antenna was designed and simulated in an IE3D software. The properties of the system were examined depending on the temperature level, type of package which contains the studied objects and the type of antenna substrate.

Keywords: RFID, temperature sensor, printed antenna, screen printing, printed electronics

1. Introduction

Temperature control is a crucial process in transportation of food or other temperature-sensitive products. When the temperature level is too high these goods can go bad and their manufacturers suffer loss [1]. In a lot of cases, indicators are used to avoid such situations. The color is changing when a product is exposed to elevated temperature.

Due to many drawbacks of such temperature indicators, i.e. optical method of state verification, other systems were designed. One of them was presented by Yang et al. [2]. The elaborated wireless sensor transmitter comprised an ink-jet printed antenna, temperature sensor, battery, quartz oscillator, integrated circuit, LED and trigger switch. Thus, the cost of this system was relatively high and its lifetime depended on battery working time.

The temperature control system demonstrated by Qiao et al. [3] used an RFID sensor in which a water pocket was integrated into the antenna substrate as a sensing unit. The electrical properties of water vary with temperature changes and in effect, antenna operation is altering and the temperature level can be calculated. A similar system was also described by Virtanen et al. [4].

There are also temperature sensors based on surface acoustic wave (SAW) RFID tags. The sensor presented by Saldanha and Malocha [5] used new pseudo-orthogonal frequency coding and makes possible to determine temperature wirelessly. Another SAW temperature sensor system demonstrated by Binder and Fachberger [6] was designed for application in high-speed high-voltage motors. It uses the dependence of signal's delay time on temperature.

Another type of the chipless RFID temperature sensor was based also on cascaded spiral resonators coupled with a microstrip connected to an antenna [7]. A temperature-dependent high K polyamide was used as the substrate of a particular spiral. Its permittivity was changing under the influence of temperature and affected the capacitance of the resonator. The resonant frequency of the spiral calculated from the Thompson equation resembled the temperature variation.

Other solution of a temperature control was proposed by Guerin et al. [8]. Their idea was based on the resistance change of a platinum deposited sensor under the influence of temperature what was combined with the frequency of a backscattering modulated signal.

All the mentioned sensor systems usually consist of many electronic components or require complicated data processing and therefore, their application results in high unit cost. Furthermore, a wide variety of products, in particular food, needs low-cost and disposable temperature sensors which are thrown away together with the package. Taking these requirements into account, this paper aims at the investigation of a disposable passive UHF RFID-enabled sensor system for detection of product's exposure to elevated temperature. An UHF antenna was designed in IE3D software and manufactured using screen printed method and further its parameters were measured with a differential probe connected to a vector network analyzer. A chip was assembled to the antenna with an isotropic conductive adhesive and finally a temperature sensitive SnBiIn alloy was deposited in the antenna circuit. The properties of the elaborated sensor system were examined depending on the temperature level, the type of substrate used for antenna printing, type of objects subjected to temperature control and sensor location (inside or outside the object under temperature control).

2. Experimental

2.1. Materials

The substrate and conductive materials used in the study are presented in Table 1. CA/CNT paste was prepared by the authors by mixing an isotropic conductive adhesive Ecolit 3654 (Panacol) with 0.5 wt% of multi-wall carbon nanotubes (CheapTubes.com) [10].

Tab. 1. Substrate and conductive materials used in the investigations.

Element of RFID sensor	Used materials
substrate	photo paper Everyday 180 g/m^2 (150 μm^a), Kapton foil HN500 (125 μm^a)
antenna	commercial silver paste PM-406
chip pads	conductive adhesive CA/CNT with an 0.5 wt% of multi-wall carbon nanotubes
chip encapsulation	low melting adhesive 3762-LM
temperature sensitive unit	low melting SnBiIn solder alloy, Kapton foil HN500 (125 μm^a), adhesive tape

[a] substrate thickness

2.2. Sample preparation

The process of RFID-enabled sensor preparation comprised four stages (Fig. 1). First, the antenna was screen printed on a flexible substrate (dimensions 50 x 80 mm) with a silver paste through a 68T polyester mesh screen and the pattern was cured in 120°C for 15 min. Next, the chip pads (dimensions 1 x 1 mm) were screen printed with CA/CNT conductive adhesive on the edges of the antenna pattern. The chip joints were created during the curing process at 120°C for 10 min and then the chip was encapsulated with the low melting adhesive. Finally, low melting SnBiIn alloy was deposited on the antenna edges and then

www.czasopisma.pan.pl   PAN   www.journals.pan.pl
POLSKA AKADEMIA NAUK

Metrol. Meas. Syst., Vol. XX (2013), No. 4, pp. 591–600.

covered with a Kapton foil. To verify the repeatability of the results six samples were prepared for each experiment.
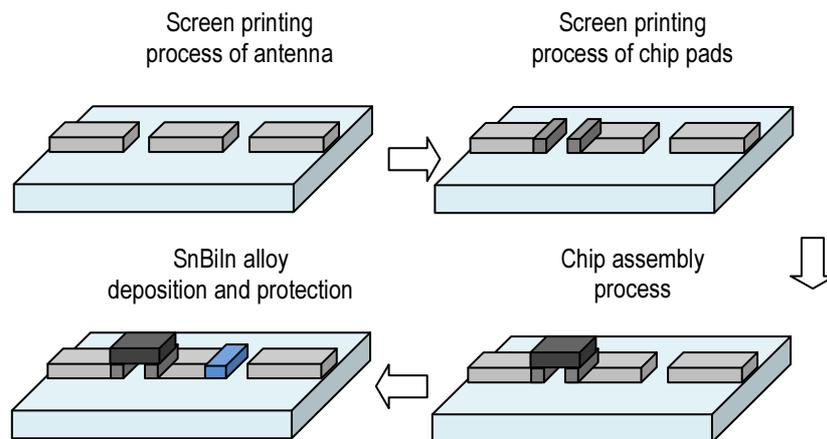

Fig. 1. Process flow to fabricate a test sample.

2.3. Measurements

2.3.1. Antenna simulation and measurements

The UHF dipole antenna of the investigated sensor was designed in the IE3D simulation software using a meandering technique described by Marrocco [11]. It was assumed that the antenna layer had a conductivity of 4.6 MS/m and a thickness of 16 μm. The substrate material had the following parameters: relative permittivity of 3.5, dissipation factor of 0.0026 and thickness of 125 μm.

The designed dipole (Fig. 2) had dimensions of 40 x 75 mm. Its main part was a meander line structure which created distributed capacitive and inductive reactances (Fig. 3) and allowed to achieve the impedance matching between the antenna and chip. The adjacent vertical lines of this meander could be associated with losses and storage of energy, whereas the horizontal lines affected the antenna radiation resistance and the total conductor length influenced the antenna inductance. The use of the meandered structure made also possible to reduce the size of the designed antenna, at the expense of lower efficiency and a narrower bandwidth compared to the straight dipole of the same height [11, 12].
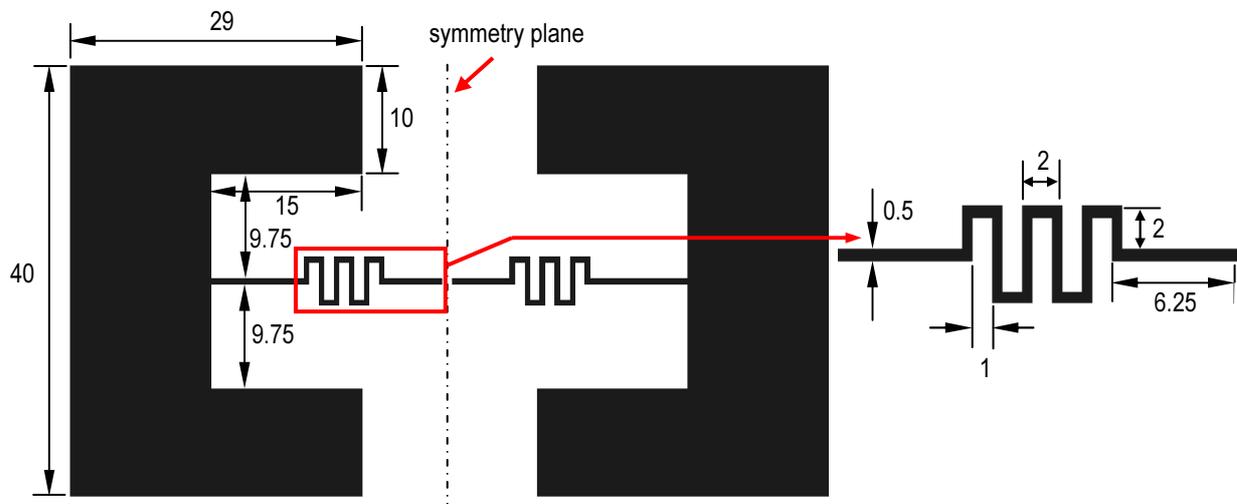

Fig. 2. Dimensions (in mm) of the designed dipole antenna.

The simulated reflection coefficient (PRC) of the designed antenna was measured in the frequency range of 0.5 - 1.5 GHz using a probe presented by Qing et al. [13]. The results of these measurements will be used to determine the antenna bandwidth and resonant frequency.
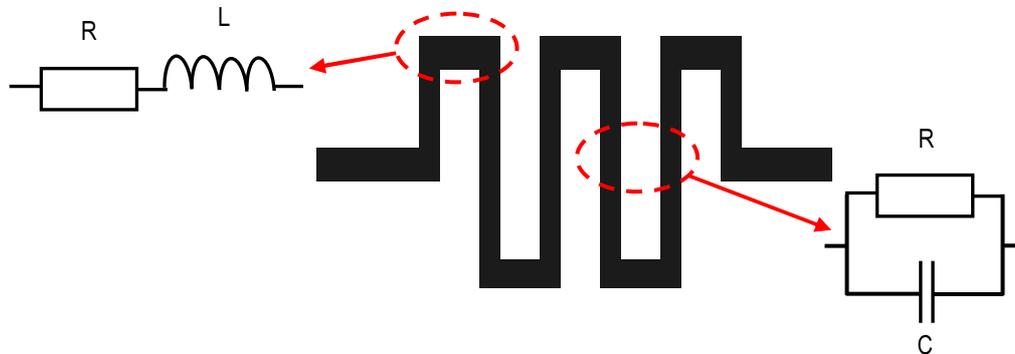

Fig. 3. Distributed capacitive and inductive reactances produced in a meander line structure.

The simulated and measured antenna reflection coefficients were determined for the chip impedance $Z_{ch} = 32 – 216j\ \Omega$. Its value corresponds to the impedance of the commercial chip Impinj Monza 3 for the frequency of 915 MHz.

2.3.2. Response time

Response time was defined as the time after which the value of sensor's resistance decreases from infinity to a few ohms. To measure them a sensor sample was placed in an oven KBC-25 heated up to a specified temperature level and its resistance was measured by multimeter Agilent 34401A (Fig. 4) connected to a computer. The measurement results were saved in an Excel worksheet to make their analysis easier. The accuracy of response time measurements was equal to ±1 s.
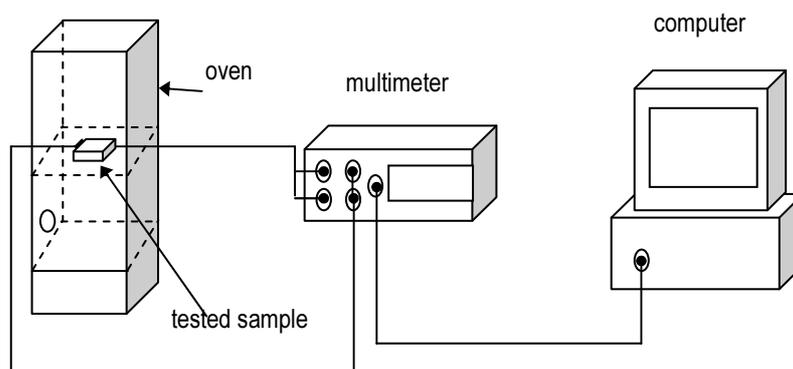

Fig. 4. The scheme of a measurement system for evaluation of the sensor response time.

2.3.3. Maximum read distance

The maximum read distance (MRD) of the fabricated sensor was measured using a system comprised of an RFID tt-8300 reader, a table moving in the horizontal plane, the object subjected to temperature and a measuring tape (Fig. 5). The acquisition of data written in the chip occurred when the controlled object approached the reader. At this moment the value of MRD was measured (Fig. 6). The accuracy of MRD measurements was ±1 cm.
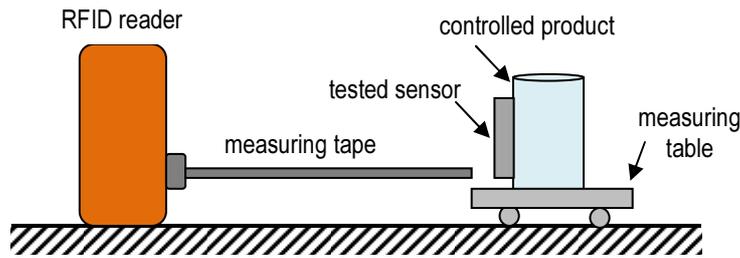
Fig. 5. The stand for measurements of the sensor's maximum read distance.

Fig. 6. The visualization of reading of electronic product code during the measurements of MRD.

3. Operation principle

The operation principle of the designed sensor system is based on altering of RFID tag's operation throughout impedance matching. This results in a change of the power transferred between the tag antenna and RFID chip (1) [4, 9] :

$$P_c(T) = \frac{4 R_c R_a}{\left| Z_c + Z_a(T) \right|^2} P_a,$$

(1)

where: T – temperature, P_c – the amount of power absorbed by the RFID chip, P_a – the maximum available power from the tag antenna, R_c – chip resistance, R_a – antenna resistance, Z_c – chip impedance, $Z_a(T)$ – temperature-dependent impedance of the tag antenna.

In the initial state, i.e. before product's exposure to elevated temperature, the tag antenna circuit is opened (2) which means that the power transferred from the antenna to the RFID chip is negligible. The construction of the designed temperature sensor generates a force F_d (Fig. 7a) which impacts on the SnBiIn alloy (3). The force F_o expresses a resistance of the alloy (3) to the foil (4). The value of F_d is lower than F_o at a temperature below 58°C. When the ambient temperature exceeds this value the state of the SnBiIn material is changing from solid to liquid and the value of F_o decreases rapidly and becomes lower than the force F_d. In the effect, the SnBiIn alloy is spreading and a connection between the antenna edges (2) is created (Fig. 7b). This causes a rapid improvement in the power transfer from antenna to chip what can be interpreted as exposure of the identified products to elevated temperature.
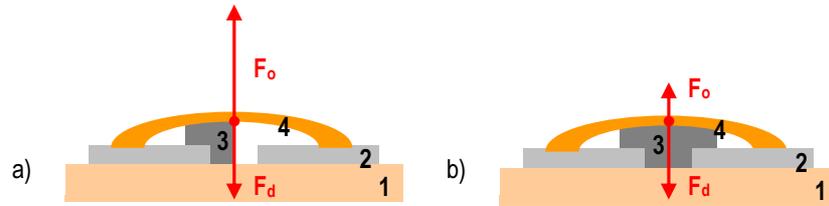
Fig. 7. The scheme of the sensor system before (a) and after (b) exposure to temperature above 58°C.

4. Results and discussion

4.1. Antenna reflection coefficient

The antenna resonant frequency determined from the simulated and measured reflection coefficient (PRC) (Fig. 8) was 915 MHz and 872.5 MHz, relatively. The type of probe used could be the reason of this differences. Further, the assumed electrical parameters of the substrate material were probably underestimated.
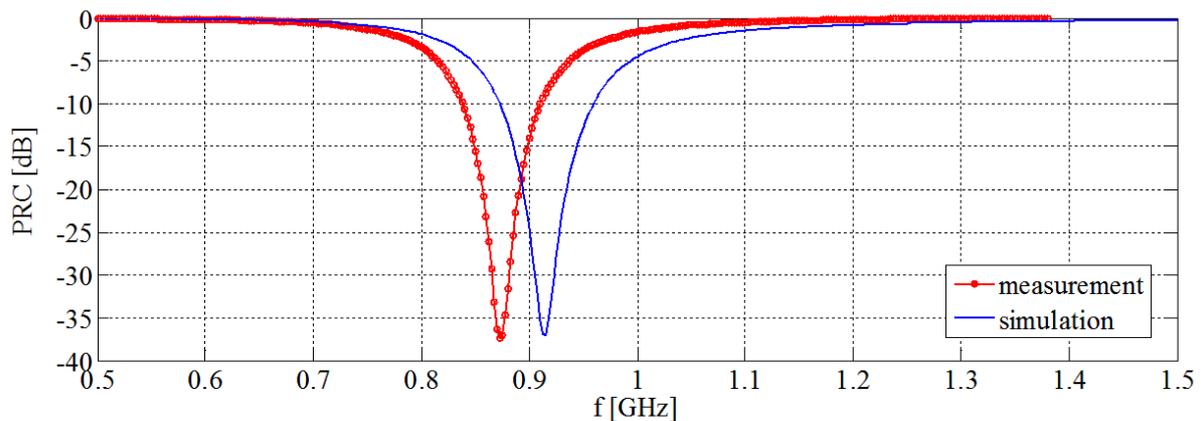

Fig. 8. The simulated and measured reflection coefficient against frequency.

Based on the achieved simulation and measurement results the antenna bandwidth was 205 MHz and 165 MHz, respectively. In the effect, it fully covered the universal UHF frequency band (860 - 960 MHz).

4.2. Response time

The response time of the sensor system was determined for a temperature of 70°C, 80°C, 100°C, and 120°C. It was noticed that higher temperature caused shorter response time (t_r) of the sensor (Fig. 9). It is because the SnBiIn solder alloy was heated up in a shorter period of time and its transformation from solid to liquid state occurred faster. In consequence, the antenna and chip circuits were connected faster, the resistance value decreased suddenly and this means that the object was exposed to elevated temperature.

The results revealed a negligible effect of the type of substrate used on the response time of the measured sensor.
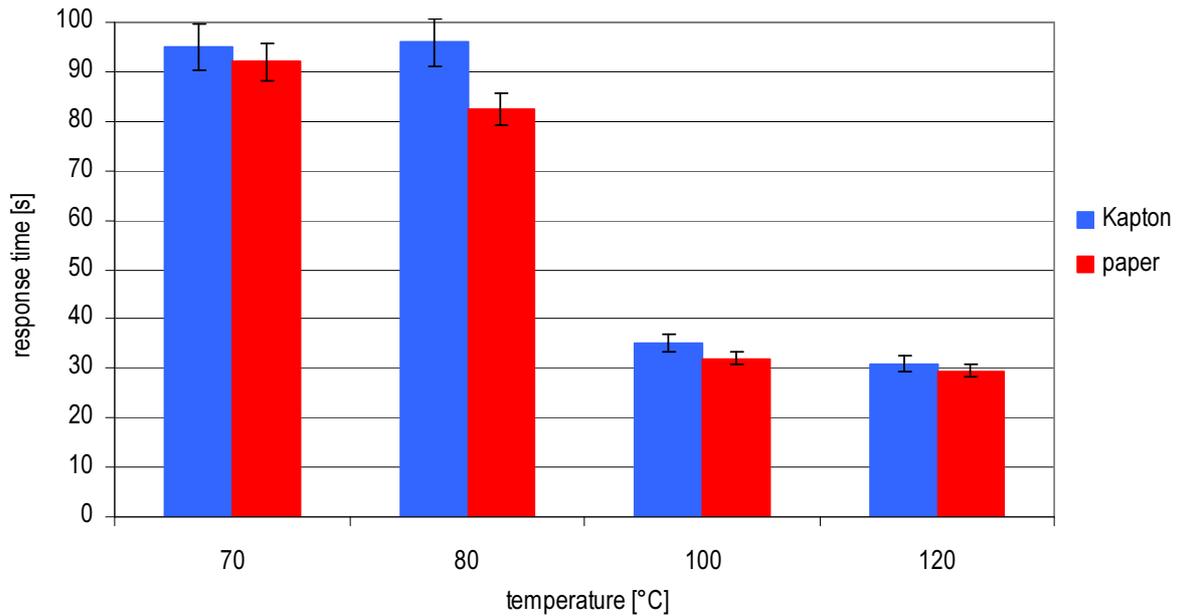
Fig. 9. The response time of the tested sensors depending on the temperature level and type of substrate used.

In Table 2 the response time values of the tested sensors applied inside or outside of a paper, glass, wood or plastic package (Fig. 10) were compared. The response time of the sensor system placed inside a package increased. It was connected with the necessity to heat up first of all the package and the air inside them.

The value of tr measured for the sensors inside a glass package was about six times higher and this value was the highest for the tested packages.For other packages the value of the response time increased approximately two times. Therefore, in the application of the designed system attention should be paid to the type of package.

Tab. 2. The response time of the sensors fabricated on paper and foil and applied inside or outside different types of packages.

Type of package	Sensors made on Kapton		Sensors made on paper	
	inside package	outside package	inside package	outside package
paper	200 ± 25	95 ± 5	166 ± 26	83 ± 8
glass	551 ± 19	91 ± 5	485 ± 23	82 ± 6
wood	254 ± 11	92 ± 7	232 ± 17	87 ± 5
plastic	256 ± 7	94 ± 4	295 ± 19	81 ± 9

4.3. Maximum read distance

The measured maximum read distance (MRD) varied from 36 cm to 80 cm (Tab. 3) and depended on the type of package. The lowest value of MRD was achieved for the glass package and the largest MRD for the wood once. This was the result of the highest attenuation of electromagnetic waves introduced by glass compared to other tested package materials.

Tab. 3. The value of maximum read distance depending on the type of package.

Type of package	MRD [cm]
glass	36 - 40
plastic	54 - 61
wood	63 - 72
free space	75 - 80

The measured maximum read distance as a function of the read angle was presented in Figures 10 and 11 for the sensor fabricated on paper and foil, relatively. In the read angle ranges of 0° - 80° and 280° - 360° the values of MRD were larger than in the range of 100° - 260° because of the attenuation of electromagnetic waves caused by packages. The MRD diagrams were 8-shaped and resulted from the polar pattern of the designed dipole antenna. Moreover, according to the previous studies [14] the maximum read distance can vary depending on the type of liquid contained in identified bottles. Therefore, in the application of the designed sensor system in logistics the type of package and its content should be taken into account.
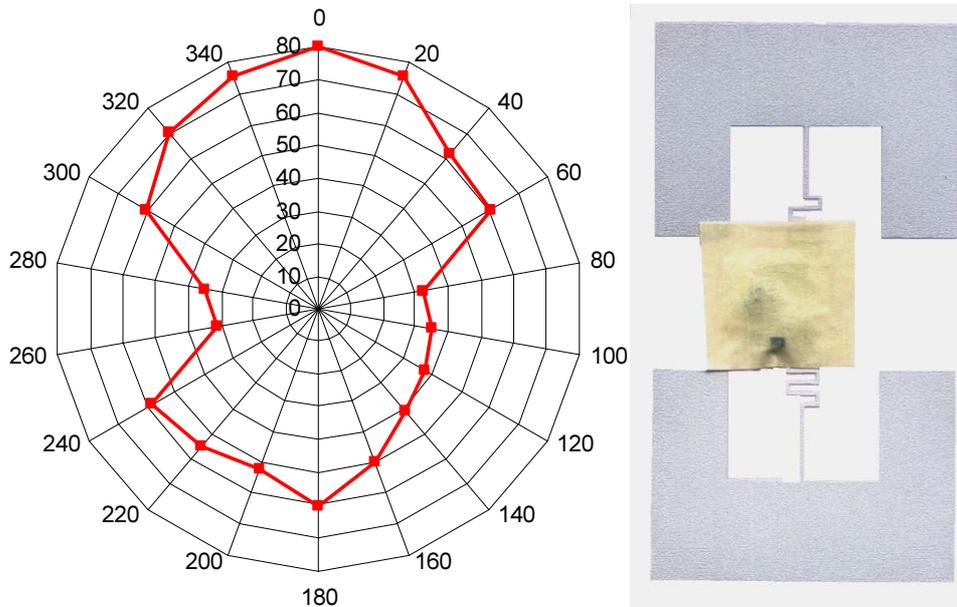

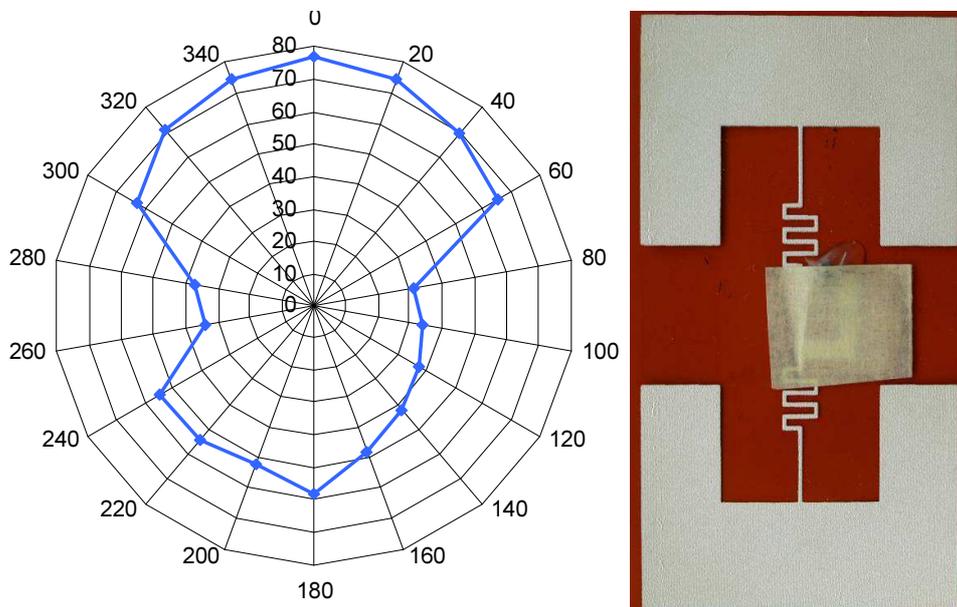Fig. 10. The diagram of the maximum read distance for the sensor system fabricated on paper.

Fig. 11. The diagram of the maximum read distance for the sensor system fabricated on Kapton.

5. Summary

In this paper, a disposable passive UHF RFID-enabled sensor system for detection of product's exposure to elevated temperature (from 58ºC up to the temperature level determined from thermal durability of the materials used) was presented. The system comprised a screen-printed UHF antenna, an RFID chip assembled with isotropic conductive adhesive with the addition of multi-wall carbon nanotubes and a temperature-sensitive unit built from SnBiIn alloy.

It was found that the response time of the sensor depended on the type of substrate used and the place where the sensor was applied. Its value was lower when the system was fabricated on paper compared to Kapton foil. Further, the response time decreased with temperature rise in a non-linear way.

The maximum read distance (MRD) of the presented system varied from 36 cm to 80 cm. The largest value of MRD was achieved for wood packages and the lowest one for glass packages because of their different attenuation of electromagnetic waves. The diagrams of MRD resembled the polar pattern of the designed dipole antenna.

Acknowledgments

References

[1] Janeczek, K., Jakubowska, M., Młożniak, A., Kozioł, G. (2012). Thermal characterization of screen printed conductive pastes for RFID antennas. *Mat Sci Eng B-Solid*, 177(15), 1336−1342.

[2] Yang, L., Vyas, R., Rida, A., Pan, J., Tentzeris, M.M. (2008). Wearable RFID-enabled sensor nodes for biomedical applications. *Proc. of 58th Electronic Components and Technology Conference*, Greenwich, Great Britain, 2156−2159.

[3] Qiao, Q., Yang, F., Elsherbeni, A.Z. (2012). Read range and sensitivity study of RFID temperature sensors. *Proc. IEEE Antennas and Propagation Society International Symposium*, Chicago, USA, 1−2.

[4] Virtanen, J., Ukkonen, L., Bjorninen, T., Sydanheimo, L., Elsherbeni, A.Z (2011). Temperature sensor tag for passive UHF RFID systems. *Proc. Sensors Applications Symposium (SAS)*, San Antonio, USA, 312−317.

[5] Saldanha, N., Malocha, D.C. (2012). Pseudo-orthogonal frequency coded wireless SAW RFID temperature sensor tags. *IEEE T Ultrason Ferr*, 59(8), 1750−1758.

[6] Binder, A., Fachberger, R. (2011). Wireless SAW Temperature Sensor System for High-Speed High-Voltage Motors. *IEEE Sens. J.*, 11(4), 996−970.

[7] Amin, E. Md., Karmakar, N. (2011). Development of a chipless RFID temperature sensor using cascaded spiral resonators. *Proc. IEEE Sensors*, Limerick, Ireland, 554−557.

[8] Guerin, M., Lauque, P., Bergeret, E., Pannier, P. (2010). A temperature and gas sensor integrated on a 915MHz RFID UHF tag. *Proc. IEEE International Conference on Wireless Information Technology and Systems (ICWITS)*, Hawaii, USA, 1−4.

[9] Cazeca, M.J., Mead, J., Chen, J., Nagarajan, R. (2013). Passive wireless displacement sensor based on RFID technology. *Sensor Actuat A-Phys*, 190, 197−202.

[10] Janeczek, K., Serzysko, T., Jakubowska, M., Koziol, G., Mlozniak, A. (2012). Mechanical durability of RFID chip joints assembled on flexible substrates. *Solder Surf Mt Tech*, 24(3) 206−215.

[11] Marrocco, G. (2008). The art of UHF RFID antenna design: impedance-matching and size-reduction techniques. *IEEE Antennas Propag*, 50(1) 66−79.

[12] Tomar, G.S., Pratap, R., Kushwah, S., Kushwah, V. (2009). Tag Antenna Analysis for RFID. *Proc. International Instrumentation and Measurement Technology Conference*, Singapore, 154−158.

[13] Qing, X., Goh, C.K., Chen, Z.N. (2009). Impedance Characterization of RFID Tag Antennas and Application in Tag Co-Design. *IEEE T Microw Theory*, 57(5) 1268−1274.

[14] Janeczek, K., Kozioł, G. (2011). Performance Characteristics of UHF RFID tags used in identification on liquids. *Przegląd Elektrotechniczny*, 5, 246−249.